Sedimentation Field-flow Fractionation: A Method for Studying Particulates in Cataractous Lens

Karin D. Caldwell,* Bruce J. Compton,* J. Calvin Giddings,* and Randall J. Olson†

It is shown that the technique of sedimentation field-flow fractionation (sedimentation [sed] FFF) can be used to determine the particle content and particle size distribution of normal and cataractous lenses. A 31-year-old normal human lens, for example, showed a particle content of 1.5% by weight with diameters ranging from 0.12 μm to 0.9 μm. The urea insoluble material present in the nuclear and cortical fractions from a densely cataractous lens contained particles ranging from 0.12 μm to 1.7 μm, with average sizes of 0.83 μm and 0.82 μm, respectively, for the two fractions. These numbers offer a basis for comparison; their actual values may be shifted slightly either up or down depending on the assessment of particle density. These sizes, which correspond to molecular weights of around 2×10^9 dalton, are larger than previously reported for lens particulates. The sed FFF method is thus seen to permit fractionation and size analysis of small amounts of lens material in times less than one hour. Invest Ophthalmol Vis Sci 25:153–159, 1984

One mechanism for human cataract formation has been felt to be polymerization of low molecular weight lens proteins.[1] As these aggregates become larger and more numerous, they must successively scatter more light impinging on the lens, ultimately causing an incapacitating lens opacification. Polymerization of lens protein occurs as a natural result of aging,[2-4] with neonates showing virtually total absence of water insoluble lens material; soluble high molecular weight (HMW) components are also absent. Normal juvenile lenses show HMW contents of less than 1% of their total soluble protein, whereas this content increases with age reaching a level of around 10% of total soluble protein in individuals fifty years or older. This HMW fraction has been shown to contain molecular weights in excess of 5×10^7 dalton.[5]

With age, the lens also develops a significant content of protein aggregates which are insoluble both in physiological (aqueous) buffers and buffers in rich in urea. Advanced cataractous lenses show over 30% by weight of urea-insoluble (UI) material.[6] It is evident that these aggregates are held together by covalent bonds rather than by loose associations such as hydrogen bonds or hydrophobic interactions.

Whereas numerous reports describe analysis of molecular size distributions seen among the soluble lens components, using such methods as gel permeation chromatography,[4] gel electrophoresis,[7] or light scattering,[5] little is known regarding the size of the insoluble protein clusters which are present in low concentration in the normal aged lens, and abundantly so in the cataractous lens.

Sedimentation field-flow fractionation (sedimentation [sed] FFF) is a one phase separation technique that is particularly well suited for the fractionation and size determination of colloidal materials. Recently, the technique has been applied to the sizing of monodisperse[8,9] and polydisperse[10] latex samples, virus particles,[11,12] bead polymerized serum albumin,[13] emulsions for intravenous nutrition,[14] and milk in various stages of aging.[15] The one-phase nature of the separation minimizes interfacial adsorption, and the open and well defined channel geometry does not restrict the size of analyzable particles in the same manner as, eg, a gel permeation column.

Although there is no inherent lower limit to the molecular weight of samples which can be analyzed by the sed FFF technique, there are some real limits posed by the seals between the spinning and stationary parts of the equipment. The nature of the system's resolving power is such that the lower the sample molecular weight, the higher is the field needed to retain and characterize the sample. Too high spin rates, however, cause the seals to leak and our current resolution limit lies around molecular weights of 2×10^7 dalton. In a unit constructed by Kirkland et al,[16] at DuPont
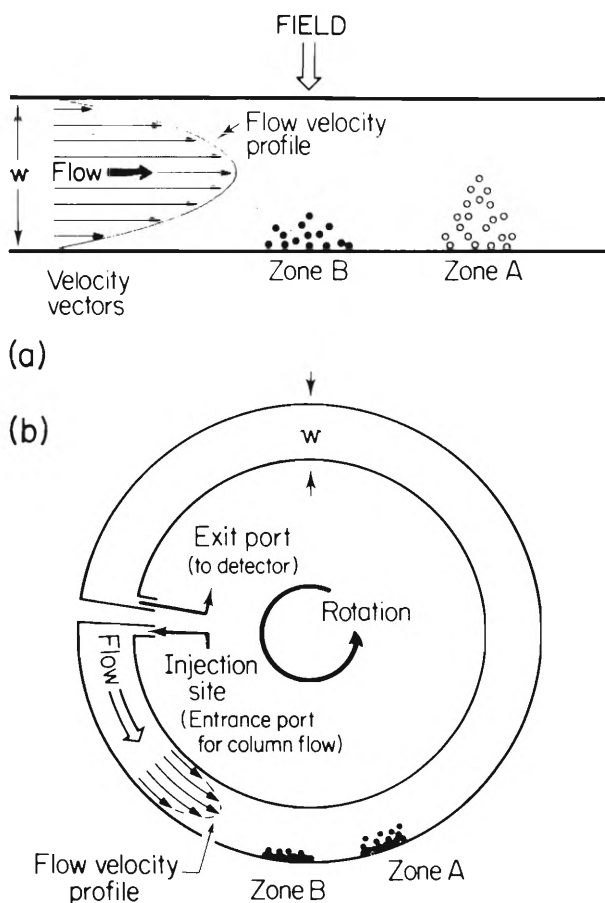
Fig. 1. Hypothetical situation in a short segment of a sed FFF channel during analysis. The particles in Zone A are either smaller, and thus faster diffusing, and/or differing less in density from the solvent than particles in Zone B. Since Zone A is less compressed by the field, it moves faster than B because it is carried by faster, more central flow lines. Both types of particles are represented here as settling to the outer wall under the field, indicating a density larger than the solvent's; a totally symmetrical situation would arise for particles less dense than the solvent, which would accumulate near the inner wall. Principle of sed FFF. The thin (w = 0.0254 cm) ribbon-like channel is curved to fit the inside of a centrifuge basket.

de Nemours Inc., the resolution limit is pushed towards molecular weights of 5×10^5 dalton.

Under the present operating condition, a particulate sample is injected into a thin ribbon-like channel through which a liquid is flowing laminarly, as shown in Figure 1. The channel, coiled to fit inside a rotor, can be spun so as to generate a field perpendicular to the direction of flow. Under the influence of the field particles in the channel will migrate towards the outer wall, provided they are denser than the liquid, or towards the inner wall if they are less dense than the carrier. The tendency to concentrate at the wall is opposed by diffusion, and at equilibrium, more or less compact layers will be formed in the wall region where fluid motion is the slowest. The layer thickness will be governed by the mass or size of sample particles such that more massive constituents are confined to thinner layers than lighter ones. Depending on the thickness of each layer, the channel flow will move the contained particles downstream at different velocities such that highly compressed layers are slower and more retained than diffuse layers. Particle separation thus occurs, and the different sized particles emerge one by one at the channel exit where they are led through a special seal into a detector.

Due to the well-defined geometry of the channel, an observed retention can be directly related by theory to the mass of the eluting particles. Resolution is high,[17] and samples with a broad spectrum of particle sizes may elute over several column volumes of liquid. In such instances it may be profitable to start the separation under conditions of high field where small particles are differentially retained. A gradual lowering of the field strength (called field programming) will then speed up sample migration and compress the elution pattern in time.[18] In this manner, small amounts of sample can be processed in runs lasting no more than an hour. Ultimately, we expect the speed to be considerably greater.

Materials and Methods

Samples

Normal and cataractous human lenses were obtained from the Division of Ophthalmology at the University of Utah Medical Center one day after removal. These were dissected according to Kramps et al,[19] in order to separate nucleus from cortex. The two types of tissue from each lens were weighed separately prior to homogenization in 1 ml of 0.1 M phosphate buffer, pH 7.5, containing 0.2 M NaCl (PBS). The homogenization was carried out by magnetic stirring overnight at 5°C. The samples were subsequently centrifuged for 4.5 min in a Beckman Microfuge to separate the supernatant, containing water soluble lens material, from the insoluble material contained in the pellet.

Supernatants were collected and immediately frozen. Pellets were resuspended in 1.25 ml PBS containing 7 M urea for a second overnight homogenization at 5°C, followed by centrifugation to separate urea soluble from urea insoluble material. This pellet, which contains the UI components, was resuspended in 1.25 ml PBS and stored frozen.

Analysis of any fraction for particle content followed thawing under constant stirring. Typical injection volumes of homogenized sample were 10–25 μl.

Equipment

The general arrangement of solvent delivery pump, FFF column, detection and recording systems is de-

picted in Figure 2. The core of this set-up is the sed FFF apparatus which has been described in detail elsewhere.[20] Its flow channel (see Fig. 1B) is 83.3 cm long, 2 cm wide, and 0.0254 cm thick (dimension labeled w in the figure) with a measured column volume (V^0) of 4.5 ml. The rotor basket, into which the channel is coiled to fit, has a radius of 7.7 cm. The gravitational acceleration G at a given rotational speed (expressed in revolutions per min, rpm) is calculated as

$$G = 7.7\left(\frac{rpm}{60}\cdot 2\pi\right)^2. \quad (1)$$

The rotational speed is under computer control, which allows field programming operation,[18] in the present case with an exponentially decaying field as described by Yau and Kirkland.[21]

Operation

The proper functioning of the sed FFF equipment is routinely checked through injection of standard particles, such as polystyrene latex spheres of known density and diameter.[8,9]

Following injection of the sample directly into the (stationary) column, the flow of carrier solvent is stopped and the centrifuge set in motion. After a 5-min stop-flow time to allow for equilibration in the channel at the desired initial field strength G_0, the flow is started and separation in the channel begins. The initial field is held constant for some time τ before it is programmed to decay exponentially according to

$$G(t) = G_0 e^{-(t-\tau)/\tau} \quad (2)$$

where G(t) is the field strength at time t after the start of flow.

The quantity of eluting particles is monitored by the detector fixed at the end of the spinning column. Particles are retained differentially in the channel due to differences in size, with small components eluting ahead of larger and more massive ones. The trace on the chart recorder then becomes a measure of the particle size distribution within a given sample, since well retained particles of diameter d are eluting at a calculable time t, such that[21]

$$\ln d = t/3\tau + \ln \beta \quad (3)$$

where

$$\beta = \left(\frac{36kT}{\pi e t^0 G_0 w\Delta\rho}\right)^{1/3} \quad (4)$$

In this expression, k symbolizes Boltzmann's constant, T the temperature in degrees Kelvin, e the base for the natural logarithm system, t^0 the time required to sweep out one column volume of liquid, G_0 the gravitational acceleration during the initial (constant field) portion of the run, w the thickness of the channel,
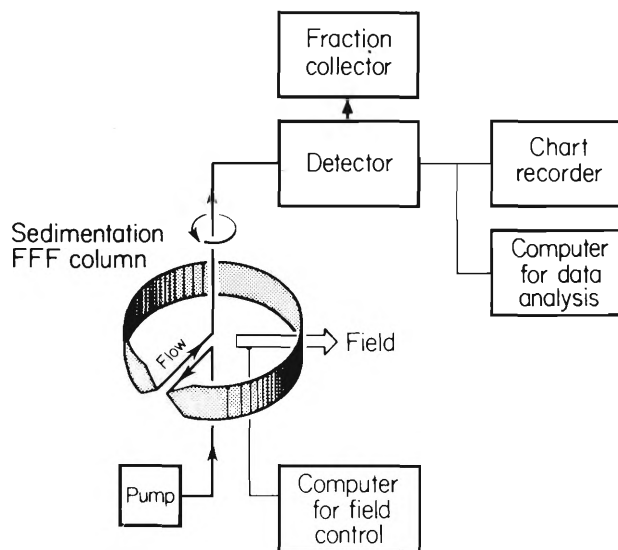

Fig. 2. General set-up of a sedimentation FFF analysis unit.

and $\Delta\rho$ the difference in density between particle and carrier.

The on-line UV detector has a 254 nm light source. Although various lens constituents absorb light at this wavelength, the main detector response to the particles is due to light scattering. This type of response is dependent on both particle concentration and size, which necessitates a correction of the response if an accurate size distribution is to be obtained from the sed FFF fractogram. Correction methods have been developed.[10,16]

Experimental Conditions

All runs in this study were performed under identical FFF conditions, with 1000 rpm as the initial field, both stop-flow time and time constant τ equal to 5 min, channel flow rate 60 ml/hr, and a T of 298K. Densities of proteins other than lipoproteins tend to range from 1.25–1.50 g/cm³. Assuming a typical value of 1.36 g/cm³ (such as for serum albumin and γ-globulin[22]) for the lens particles, $\Delta\rho$ is taken as 0.36 g/cm³. More accurate determinations could be obtained if the density of the particles were precisely known. Exact density evaluations are difficult to carry out; the purpose of the present study is to demonstrate "fingerprinting" of the particle size distribution in materials of similar origin by sed FFF and an exact value for the particle density is not required. However, if this density were determined to be as low as 1.20 g/cm³ the present particle size scales in Figures 3–6 should be multiplied by the factor 1.22 (as seen from equations 3 and 4). Conversely, if the actual particle density proved to be 1.50 g/cm³ the diameter scales should be reduced to 0.9 of their present level. The only variable in the
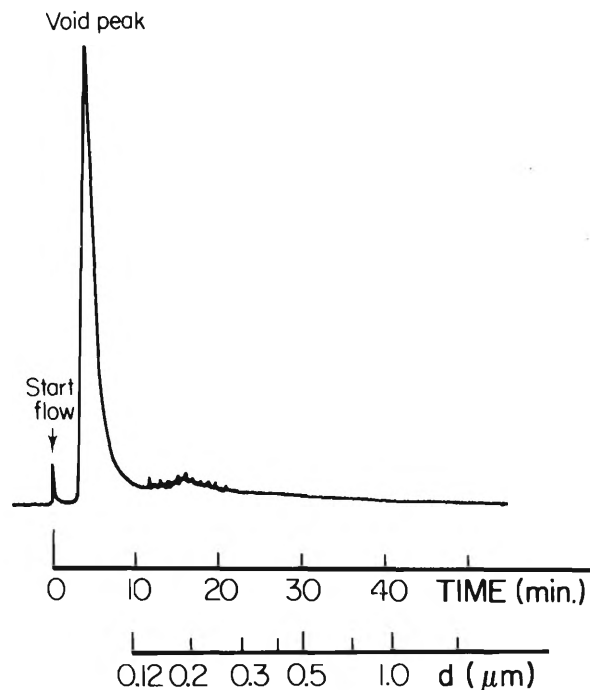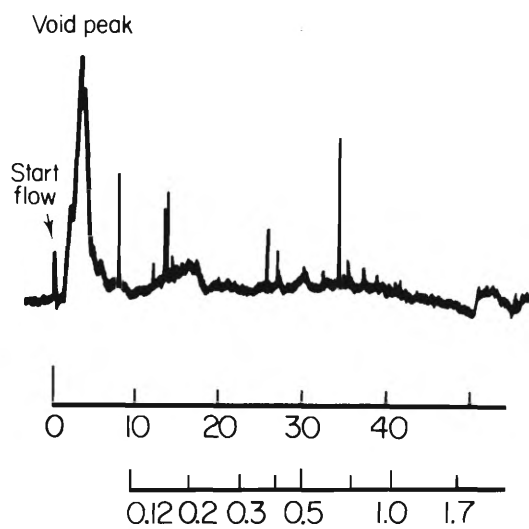
Void peak

Start
flow

0   10   20   30   40   TIME (min.)

0.12 0.2 0.3 0.5   1.0   d (μm)

Fig. 3. Particle size distribution in the homogenate from a whole normal 31-year-old human lens as reflected by sedimentation FFF. The field, initially held at 1000 rpm, was decayed with a time constant of 5 min; the flow rate was 1 ml/min. The void peak has a maximum of 0.18 absorbance units.
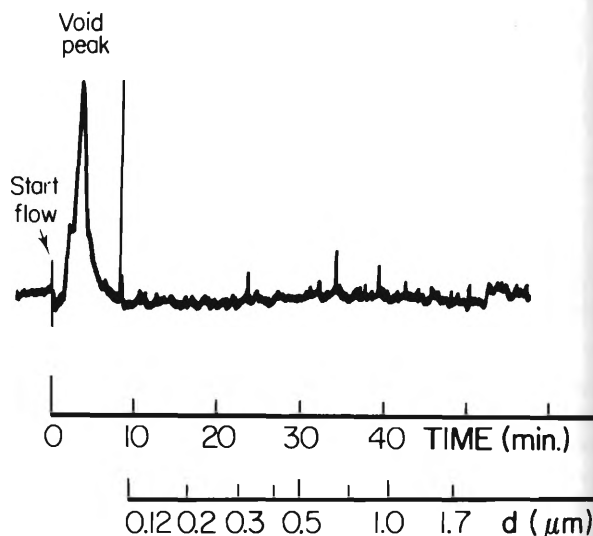
system was detector sensitivity, which was changed as an adjustment to the concentration of particles present.

Data Evaluation

The raw fractograms were examined to identify the void peak, which contains all particles and macro-

molecules small enough to be unaffected by the centrifugal field as they pass through the channel. The elution time for this unretained peak is symbolized by t^0 in equation 4. Since the chart paper moves forward at a constant rate, distances on the chart are proportional to time and equation 3 permits establishment of a particle diameter scale directly onto the fractogram.

The detector response A at any given diameter d must be corrected for its size dependence[10] in order to yield a true concentration distribution. Measured chart distances from the start of the run are converted to time and fed into a computer together with the corrected detector response corresponding to this elution time. Through moment analysis[23] one may compute the area under the retained peak—which reflects the total concentration of retained particles—and the center of the peak, reflecting the average diameter of retained particles. In this context "retained particles" are particles emerging after completed elution of the void (or unretained) peak.

Results

By adhering to a fixed set of experimental conditions, the FFF fractograms become directly comparable for a rapid evaluation of similarities or differences in the particle content of the various fractions. In performing this comparison, however, allowance must be made for differences in weight of the different sample tissues. Since each sample was homogenized in a given volume of buffer, the concentration of lens material in each homogenate is proportional to the initial weight of the sample.

Void peak

Start
flow

0   10   20   30   40

0.12 0.2 0.3 0.5   1.0   1.7

(a)

Void peak

Start
flow

0   10   20   30   40   TIME (min.)

0.12 0.2 0.3 0.5   1.0   1.7   d (μm)

(b)

Fig. 4. Sedimentation FFF fractograms of the urea insoluble material in normal 15-year-old human lens, deriving from **a,** nucleus and **b,** cortex. The void peak in each case has a maximum of 0.005 absorbance units. No retained peak, and thus no significant particle content is detected in either fraction. (The spikes represent noise at this high detector sensitivity.)

Figure 3 shows a typical fractogram obtained from the homogenized, normal, whole lens of a 31-year-old man. The trace thus represents the original distribution of particles, ie, both urea soluble and insoluble, which is present in the lens. Significant features in this elution trace are the void peak, which contains all soluble components with UV absorption at 254 nm, as well as suspended particles small enough to remain uniformly distributed across the channel even in the presence of the field. A particle diameter scale is superimposed on the fractogram, in accordance with equation 3 of the experimental section. In view of the poor resolution of sizes in the void or near void region, it is meaningless to extend this scale to V^0. We have chosen to consider a diameter d of 0.12 μm as the smallest reliably determined size under the presently selected experimental conditions. With the help of the particle size scale shown on the figure, we may identify the broad, low amplitude, retained peak as consisting of particles with diameters varying from about 0.12 μm to 0.9 μm with a maximum abundance at 0.19 μm. From measurement of the area under the retained peak, the particle content of this lens is estimated to be about 1.5% of its total wet weight.

The standard way in which we treated most lenses is outlined in the experimental section. Homogeni-
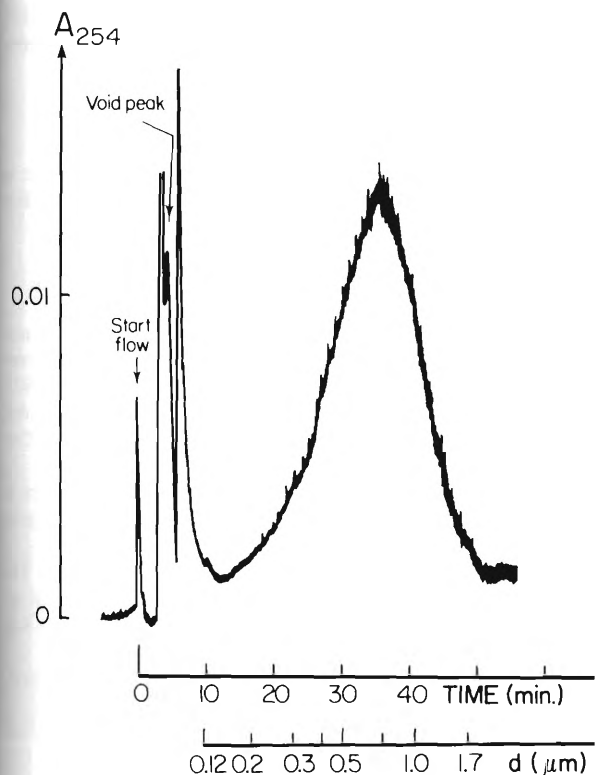

Fig. 5. Sedimentation FFF fractogram of urea insoluble material from the nucleus of a cataractous human lens. The absorbance maximum for the retained peak (corresponding to particulate material) is 0.012 absorbance units.
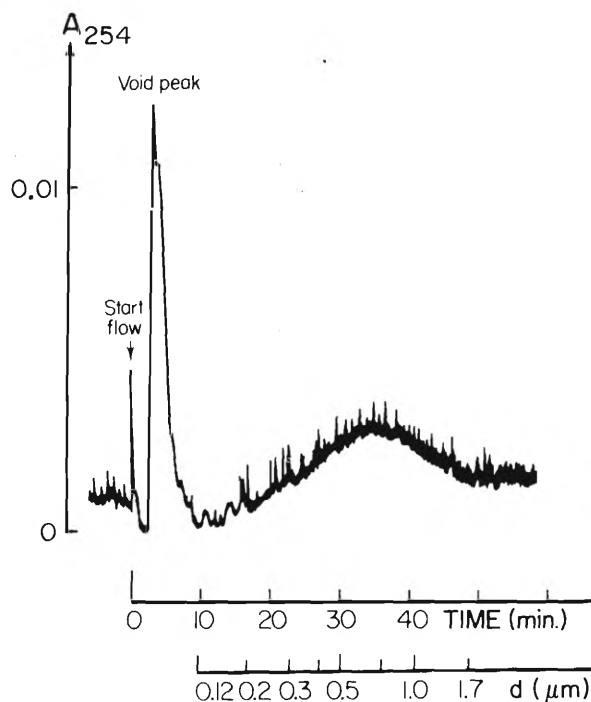

Fig. 6. Sedimentation FFF fractogram of urea insoluble material from the cortex of a cataractous human lens. The absorbance maximum for the retained peak is 0.002 absorbance units.

zation of the nuclear and cortical portions of the lens was followed by centrifugation to recover water insoluble particles. These were subsequently homogenized in urea containing buffer for solubilization of noncovalently linked material, and the remaining particles were spun down and recovered as the UI fraction. The various solubilization procedures left only minute amounts of particles in the UI fraction from nucleus and cortex of a 15-year-old in Figure 4. In spite of injection volumes of 100 μl (8% of the total UI fraction of the sample) and a 16-fold increase in detector sensitivity, as compared with Figure 3, there is no demonstrable particle content in the fractions from either the nucleus or cortex. A "blank" injection of 100 μl suspension medium showed the baseline noise to be commensurate with the results of Figure 4 at the high detector sensitivity used.

As expected, the particle contents of UI fractions from cataractous lenses are significantly different from those of young normal lenses. Figures 5 and 6 demonstrate fractograms from the nuclear and cortical cuts of a densely cataractous lens from a 75-year-old that upon visual inspection appeared to have a black nucleus and brown cortex. The wet weight of the dissected nucleus was 51 mg versus 136 mg for the cortex, but despite this weight difference (and the resulting difference in concentration of the initial homogenates), identical injected volumes of respective UI fractions showed a larger particle content (represented by the four times larger peak area) in the nuclear than in the

cortical fraction. Thus this nucleus contains approximately 10 times as much particles per unit wet weight as does the cortex. The size distribution, however, appears quite similar in the two fractions, with maxima occurring for particles 0.65 μm (nucleus) and 0.61 μm (cortex) in diameter; the center of gravity for each peak, which represents the weight average particle diameter for that material, occurs at 0.83 μm and 0.82 μm, respectively. These values would be altered slightly upon application of a light scattering correction to remove the particle size dependence from the detector response. The entire problem with detector corrections can be avoided if the particles are known to be of a uniform composition. In this type of case, a chemical assay of the effluent from the fractionation will give a correct representation of the sample's particle size distribution.

A number of other lenses were examined. They all had less severe opacity and showed lower total particle contents as well as smaller particle diameters at the distribution maxima than the lens in Figures 5 and 6.

Discussion

The chemical background to the polymerization of lens protein has received much attention in the last decade. Among the moderately high molecular weight aggregates that form in the lens during aging, some exist that are entirely held together by noncovalent bonds.[7,24] These aggregates become soluble upon addition of urea. By contrast, the UI fractions from both normal and cataractous lenses show high contents of disulfide linkages.[3,25] Following reduction and alkylation, this UI material shows similar composition as the urea soluble fraction.[7] In view of this and similar findings, Truscott and Augusteyn[6] proposed the existence of some mechanism in the normal lens which functions to keep its proteins in a reduced state. Hata and Hockwin[26] found antioxidants, such as glutathione and ascorbate, to be unevenly distributed in the lens, with higher concentrations in the cortex than in the nucleus. This finding parallels the commonly observed higher particle concentrations in the nucleus as compared with cortex, which is also demonstrated by the sed FFF results presented here. It should be mentioned that lens membrane components being UI and lipid-rich may be missed by sed FFF if their density equals that of the carrier. Their oxidation may be an important event as well in cataractogenesis.

Formation of disulfide linkages appears to be only one of a number of oxidation reactions within the lens that lead to protein polymerization and lens opacity. The tyrosine and tryptophan residues of certain lens proteins have been shown to undergo chemical changes as a result of exposure to UV irradiation.[27,28] In an *in vitro* experiment, Buckingham and Pirie[29] were able to induce crosslinking of lens crystallins through irradiation by sunlight. Zigler et al[30,31] also demonstrated crosslinking of crystallins following irradiation *in vitro*. In the presence of certain dyes which acted as photosensitizing agents, the polymerization was enhanced. Totally deoxygenated solutions showed no polymerization, implying singlet oxygen as a reactive intermediate in the photoinduced polymerization. In a separate experiment, non-dye-mediated singlet oxygen production had the same polymerizing effect on crystallins in the absence of reducing agents. Polymerization produces a yellowing of the protein, a reduction of its tryptophan content, and an observable shift in the crystallin fluorescence spectrum.[29] Oxidation of tryptophan is known to produce N-formylkynurenine; kynurenines are found in human lens[32,33] where their known photosensitizing properties[34,35] could result in polymerization of crystallins.

The insoluble protein fraction from human lens is believed to contain the most highly modified crystallins, in view of its strong pigmentation, blue fluorescence, and high content of covalent crosslinks. By analyzing the growth pattern of lens particulates and by comparing crosslinking patterns for particles of different size within one and the same lens, it is hoped that further light might be shed on the mechanism of cataract formation.

References

1. Buckingham RH: The behaviour of reduced proteins from normal and cataractous lenses in highly dissociating media: crosslinked protein in cataractous lenses. Exp Eye Res 14:123, 1972.
2. Anderson EI, Wright DD, and Spector A: The state of sulfhydryl groups in normal and cataractous human lens proteins. II. Cortical and nuclear regions. Exp Eye Res 29:233, 1979.
3. Anderson EI and Spector A: The state of sulfhydryl groups in normal and cataractous human lens proteins. I. Nuclear region. Exp Eye Res 26:407, 1978.
4. Jedziniak JA, Kinoshita JH, Yates EM, and Benedek GB: The concentration and localization of heavy molecular weight aggregates in aging normal and cataractous human lenses. Exp Eye Res 20:367, 1975.
5. Benedek GB: Theory of transparency of the eye. Appl Opt 10:459, 1971.
6. Truscott RJW and Augusteyn RC: The state of sulfhydryl groups in normal and cataractous human lenses. Exp Eye Res 25:139, 1977.
7. Roy D and Spector A: Human insoluble lens protein. I. Separation and partial characterization of polypeptides. Exp Eye Res 26:429, 1978.
8. Karaiskakis G, Myers MN, Caldwell KD, and Giddings JC:

Verificat
imentati
9. Gidding
Colloid
ation. I.
1983.
10. Yang FS
by sedin
tributior
11. Caldwel
Field-flo
virus fr
Method
12. Caldwel
of T4D
matogr
13. Caldwel
Charact
flow fra
14. Yang F
characte
Emulsi
15. Yang F
fraction
16. Kirklan
ponenti
ation fo
1981.
17. Gidding
parison
flow fra
1975.
18. Yang
mental
19. Kramp
in the
Biochi
20. Giddin
of bio
tionati
D, edi
21. Yau

Verification of retention and zone spreading equations in sedimentation field-flow fractionation. Anal Chem 53:1314, 1981.

9. Giddings JC, Karaiskakis G, Caldwell KD, and Myers MN: Colloid characterization by sedimentation field-flow fractionation. I. Monodisperse populations. J Colloid Interface Sci 92:66, 1983.

10. Yang FS, Caldwell KD, and Giddings JC: Colloid characterization by sedimentation field-flow fractionation. II. Particle size distribution. J Colloid Interface Sci 92:81, 1983.

11. Caldwell KD, Nguyen TT, Giddings JC, and Mazzone HM: Field-flow fractionation of alkali-liberated nuclear polyhedrosis virus from gypsy moth Lymantria dispar Linnaeus. J Virol Methods 1:241, 1980.

12. Caldwell KD, Karaiskakis G, and Giddings JC: Characterization of T4D virus by sedimentation field-flow fractionation. J Chromatogr 215:323, 1981.

13. Caldwell KD, Karaiskakis G, Myers MN, and Giddings JC: Characterization of albumin microspheres by sedimentation field-flow fractionation. J Pharm Sci 70:1350, 1981.

14. Yang FS, Caldwell KD, Myers MN, and Giddings JC: Colloid characterization by sedimentation field-flow fractionation. III. Emulsions. J Colloid Interface Sci 92:115, 1983.

15. Yang FS: Colloid characterization by sedimentation field-flow fractionation. PhD thesis, University of Utah, 1981.

16. Kirkland JJ, Rementer SW, and Yau WW: Time-delayed exponential field-programmed sedimentation field-flow fractionation for particle-size-distribution analyses. Anal Chem 53:1730, 1981.

17. Giddings JC, Yoon HY, and Myers MN: Evaluation and comparison of gel permeation chromatography and thermal field-flow fractionation for polymer separation. Anal Chem 47:126, 1975.

18. Yang FJF, Myers MN, and Giddings JC: Programmed sedimentation field-flow fractionation. Anal Chem 46:1924, 1974.

19. Kramps HA, Hoenders HJ, and Wollensak J: Protein changes in the human lens during development of sentile nuclear cataract. Biochim Biophys Acta 434:32, 1976.

20. Giddings JC, Myers MN, Caldwell KD, and Fisher SR: Analysis of biological macromolecules and particles by field-flow fractionation. In Methods of Biochemical Analysis, vol 26, Glick D, editor. New York, John Wiley & Sons, 1980, pp. 79–136.

21. Yau WW and Kirkland JJ: Retention characteristics of time-delayed exponential field-programmed sedimentation field-flow fractionation. Sep Sci Technol 16:577, 1981.

22. Sober HA (editor): Handbook of Biochemistry. Cleveland, Ohio, CRC Press, 1968, pp. C36–C39.

23. Grushka E, Myers MN, Schettler PD, and Giddings JC: Computer characterization of chromatographic peaks by plate height and higher central moments. Anal Chem 41:889, 1969.

24. Li LK and Spector A: Effects of modification of the sulfhydryl groups of calf lens low molecular weight alpha-crystallin. Exp Eye Res 26:419, 1978.

25. Spector A and Roy D: Disulfide-linked high molecular weight protein associated with human cataract. Proc Natl Acad Sci USA 75:3244, 1978.

26. Hata N and Hockwin O: Enzymatic determination of reduced and oxidized glutathione in bovine lenses of different ages and their distribution in lens equator and nucleus. Ophthalmic Res 9:256, 1977.

27. Pirie A: Color and solubility of the proteins of human cataracts. Invest Ophthalmol 7:634, 1968.

28. Garcia-Castineiras S, Dillon J, and Spector A: Non-tryptophan fluorescence associated with human lens protein: apparent complexity and isolation of bityrosine and anthranilic acid. Exp Eye Res 26:461, 1978.

29. Buckingham RH and Pirie A: The effect of light on lens proteins in vitro. Exp Eye Res 14:297, 1972.

30. Goosey JD, Zigler JS Jr, and Kinoshita JH: Cross-linking of lens crystallins in a photodynamic system: a process mediated by singlet oxygen. Science 208:1278, 1980.

31. Goosey JD, Zigler JS Jr, Matheson IBC, and Kinoshita JH: Effects of singlet oxygen on human lens crystallins in vitro. Invest Ophthalmol Vis Sci 20:679, 1981.

32. Zigman S: Near UV light and cataracts. Photochem Photobiol 26:437, 1977.

33. Dillon J, Spector A, and Nakanishi K: Identification of β-carbolines isolated from fluorescent human lens proteins. Nature 259:422, 1976.

34. Walraut P and Santus R: N-formyl-kynurenine, a tryptophan photooxidation product, as a photodynamic sensitizer. Photochem Photobiol 19:411, 1974.

35. Zigler JS and Goosey JD: Photosensitized oxidation in the ocular lens: evidence for photosensitizers endogenous to the human lens. Photochem Photobiol 33:869, 1981.